Check for updates

Received: 24 October 2023 | Revised: 21 December 2023 | Accepted: 2 January 2024

DOI: 10.1111/bph.16330

THEMED ISSUE ARTICLE

MicroRNA-guided drug discovery for mitigating persistent pulmonary complications in critical COVID-19 survivors: A longitudinal pilot study

María C. García-Hidalgo[1,2] | Iván D. Benítez[1,2] | Manel Perez-Pons[1,2] | Marta Molinero[1,2] | Thalía Belmonte[1,2] | Carlos Rodríguez-Muñoz[1,2] | María Aguilà[1] | Sally Santisteve[1,2] | Gerard Torres[2,3] | Anna Moncusí-Moix[3] | Clara Gort-Paniello[1,2] | Rafael Peláez[4] | Ignacio M. Larráyoz[4,5] | Jesús Caballero[6] | Carme Barberà[7] | Estefania Nova-Lamperti[8] | Antoni Torres[2,9] | Jessica González[1,2] | Ferran Barbé[1,2] | David de Gonzalo-Calvo[1,2]

[1]Translational Research in Respiratory Medicine, University Hospital Arnau de Vilanova and Santa Maria, IRBLleida, Lleida, Spain

[2]CIBER of Respiratory Diseases (CIBERES), Institute of Health Carlos III, Madrid, Spain

[3]Group of Precision Medicine in Chronic Diseases, University Hospital Arnau de Vilanova and Santa Maria, IRBLleida, Lleida, Spain

[4]Biomarkers and Molecular Signaling Group, Neurodegenerative Diseases Area Center for Biomedical Research of La Rioja, CIBIR, Logroño, Spain

[5]BIAS, Department of Nursing, University of La Rioja, Logroño, Spain

[6]Grup de Recerca Medicina Intensiva, Intensive Care Department Hospital Universitari Arnau de Vilanova, Lleida, Spain

[7]Intensive Care Department, University Hospital Santa María, IRBLleida, Lleida, Spain

[8]Molecular and Translational Immunology Laboratory, Department of Clinical Biochemistry and Immunology, Faculty of Pharmacy, Universidad de Concepcion, Concepcion, Chile

[9]Pneumology Department, Clinic Institute of Thorax (ICT), Hospital Clinic of Barcelona, Insitut d'Investigacions Biomèdiques August Pi i Sunyer (IDIBAPS), ICREA, University of Barcelona (UB), Barcelona, Spain

Correspondence
David de Gonzalo-Calvo, PhD, Translational Research in Respiratory Medicine, University Hospital Arnau de Vilanova and Santa Maria, IRBLleida. Avda, Alcalde Rovira Roure 80, 25198 Lleida, Spain.
Email: dgonzalo@irblleida.cat

Funding information
This work is supported by Instituto de Salud Carlos III (COV20/00110), co-funded by the European Union and Centro de Investigación Biomedica En Red – Enfermedades Respiratorias (CIBERES). CIBERES is an initiative of the Instituto de Salud Carlos III. We were further funded by Programa de donaciones "estar preparados" UNESPA

Abstract

Background and Purpose: The post-acute sequelae of SARS-CoV-2 infection pose a significant global challenge, with nearly 50% of critical COVID-19 survivors manifesting persistent lung abnormalities. The lack of understanding about the molecular mechanisms and effective treatments hampers their management. Here, we employed microRNA (miRNA) profiling to decipher the systemic molecular underpinnings of the persistent pulmonary complications.

Experimental Approach: We conducted a longitudinal investigation including 119 critical COVID-19 survivors. A comprehensive pulmonary evaluation was performed in the short-term (median = 94.0 days after hospital discharge) and long-term (median = 358 days after hospital discharge). Plasma miRNAs were quantified at the

Abbreviations: ARDS, acute respiratory distress syndrome; D_{LCO}, lung diffusing capacity for carbon monoxide; IMV, invasive mechanical ventilation; KIM1, kidney injury molecule 1; PTN, pleiotrophin.

This is an open access article under the terms of the Creative Commons Attribution-NonCommercial-NoDerivs License, which permits use and distribution in any medium, provided the original work is properly cited, the use is non-commercial and no modifications or adaptations are made.
© 2024 The Authors. *British Journal of Pharmacology* published by John Wiley & Sons Ltd on behalf of British Pharmacological Society.

(Madrid, Spain), Fundación Francisco Soria Melguizo (Madrid, Spain), Beca SEPAR – Ayuda a la investigación (1437/2023), Beca SEPAR – Ayuda a la investigación (1222/2022) and Beca SOCAP – Investigador emergent. MCGH is the recipient of a predoctoral fellowship from "Universitat de Lleida." MM is the recipient of a predoctoral fellowship (PFIS: FI21/00187) from Instituto de Salud Carlos III and co-funded by the European Union. MPP is the recipient of a predoctoral fellowship (PFIS: FI23/00022) from Instituto de Salud Carlos III and co-funded by the European Union. CR is supported by Departament de Salut (Pla Estratègic de Recerca i Innovació en Salut (PERIS): SLT028/23/000191). IML is supported by a Miguel Servet contract (CPII20/00029) from the Instituto de Salud Carlos III, co-funded by the European Union. DdGC has received financial support from Instituto de Salud Carlos III (Miguel Servet 2020: CP20/00041), co-funded by the European Union. Funders did not participate in any part of the research design, conduct, analysis and manuscript production.

short-term evaluation using the gold-standard technique, RT-qPCR. The analyses combined machine learning feature selection techniques with bioinformatic investigations. Two additional datasets were incorporated for validation.

Key Results: In the short-term, 84% of the survivors exhibited impaired lung diffusion (D_{LCO} < 80% of predicted). One year post-discharge, 54.4% of this patient subgroup still presented abnormal D_{LCO}. Four feature selection methods identified two specific miRNAs, miR-9-5p and miR-486-5p, linked to persistent lung dysfunction. The downstream experimentally validated targetome included 1473 genes, with heterogeneous enriched pathways associated with inflammation, angiogenesis and cell senescence. Validation studies using RNA-sequencing and proteomic datasets emphasized the pivotal roles of cell migration and tissue repair in persistent lung dysfunction. The repositioning potential of the miRNA targets was limited.

Conclusion and Implications: Our study reveals early mechanistic pathways contributing to persistent lung dysfunction in critical COVID-19 survivors, offering a promising approach for the development of targeted disease-modifying agents.

KEYWORDS

drug discovery, drug repositioning, long COVID, lung dysfunction, machine learning, microRNA, post-acute COVID-19 sequelae

1 | INTRODUCTION

The post-acute sequelae of SARS-CoV-2 are increasingly recognized as a global societal challenge, given their impact on individual well-being and their substantial burden on healthcare systems and the economy (Kerksieck et al., 2023). This condition encompasses a wide spectrum of multiorgan symptoms and complications that manifest following the recovery from acute COVID-19 (post-acute COVID-19 syndrome, post-COVID syndrome or long COVID). The core symptoms include persistent fatigue, anosmia, memory loss, muscle pain and respiratory difficulties, among others (Nalbandian et al., 2021). The presence of post-acute organ damage following SARS-CoV-2 infection primarily pertains to pulmonary complications (Singh et al., 2023), spanning from self-limited abnormalities to advanced-stage pulmonary pathology.

Lung dysfunction has arisen as the hallmark in convalescent individuals recovering from severe COVID-19, with the lung diffusing capacity for carbon monoxide (D_{LCO}) representing the most compromised parameter of pulmonary function in hospitalized patients. Data from various patient cohorts indicate a prevalence of impaired diffusing capacity of around 50% even 1 year after hospital discharge (Schlemmer et al., 2023). This observation aligns with findings from investigations into other coronaviruses, influenza and acute respiratory distress syndrome (ARDS) (Herridge et al., 2003). Although the number of ongoing clinical trials and therapies under development continues to grow, there are no widely accepted treatment options for managing pulmonary lesions in survivors of severe respiratory infections, including critical COVID-19. For instance, there is

What is already known

- The molecular basis of the pulmonary sequelae persistence remains unclear.
- Treating respiratory complications in post-severe infections is challenged by ineffective therapies.

What does this study add

- Plasma levels of miR-9-5p and miR-486-5p are associated with long-term lung dysfunction.
- At the systemic level, the molecular signature of persistent respiratory sequelae involves diverse pathobiological mechanisms.

What is the clinical significance

- Heterogeneity could hinder patient management, contributing to limited treatment responses and unfavourable clinical trial outcomes.
- miRNA-based therapeutics offer a promising avenue for addressing the persistence of lung dysfunction.

14765381, 0, Downloaded from https://bpspubs.onlinelibrary.wiley.com/doi/10.1111/bph.16330 by Universidad de la Rioja, Wiley Online Library on [14/03/2024]. See the Terms and Conditions (https://onlinelibrary.wiley.com/terms-and-conditions) on Wiley Online Library for rules of use; OA articles are governed by the applicable Creative Commons License

insufficient evidence to support the use of anti-fibrotic agents in resolving pulmonary fibrosis that results from infections such as SARS-CoV-2 (Mylvaganam et al., 2021). Understanding the pathobiological mechanisms contributing to the persistence of lung dysfunction after hospital discharge is therefore of paramount importance. This molecular approach would allow the development of new therapeutic strategies or the repositioning of previously approved drugs for early and targeted interventions, avoiding exposure to low-effective disease-modifying agents.

MicroRNAs (miRNAs), a class of small noncoding RNAs consisting of 19–25 nucleotides, play a pivotal role in post-transcriptional gene expression regulation by binding to target mRNAs, thereby suppressing translation and/or inducing target mRNA degradation. miRNAs form coordinated and complex gene expression networks (Makkos et al., 2021), with a single miRNA capable of targeting numerous transcripts, and a specific transcript containing binding sites for multiple miRNAs. Consequently, miRNAs are increasingly recognized as key regulators of virtually all cellular processes. Evidence from in vitro and in vivo studies underscores their contribution to disease pathogenesis, including respiratory conditions (Rupani et al., 2013). Moreover, miRNAs have been detected in the extracellular milieu and various biofluids (Valadi et al., 2007), where they participate in cell-to-cell communication, mainly through paracrine signalling (Li et al., 2021). While the concept of miRNAs acting as hormones has been a subject of debate (Bär et al., 2019), numerous studies conducted over the years have provided compelling evidence of their role as endocrine genetic signals (Ying et al., 2021).

Altogether, miRNA profiling has emerged as a promising tool for comprehensively unravelling disease mechanisms and identifying potential interventions (Jusic et al., 2022). In this study, we employed circulating miRNA profiling in conjunction with machine learning feature selection techniques to characterize, for the first time, the early mechanistic pathways associated with the persistence of lung dysfunction (1 year after hospital discharge) in survivors of critical COVID-19. The ultimate goal was to propose novel therapeutic candidates aimed at mitigating long-term pulmonary abnormalities.

2 | METHODS

2.1 | Study population

This was a substudy of the CIBERESUCICOVID multicentre study (Torres et al., 2021). Survivors of critical COVID-19 admitted to intensive care units (ICU) between March and December 2020 and subsequently evaluated in a post-COVID-19 consultation in Hospital Universitari Arnau de Vilanova-Santa María (Lleida, Spain) were enrolled if they fulfilled the following inclusion criteria: positive nasopharyngeal swab PCR for SARS-CoV-2, aged over 18, developed ARDS according to the Berlin definition (Ranieri et al., 2012) and presence of diffusion impairment in the short-term evaluation of the follow-up (defined as a D_{LCO} < 80%). The exclusion criteria included previous chronic pulmonary disease, died during the follow-up, transferred to another department or institution, incomplete follow-up and presence of non-COVID alterations that could hamper the follow-up or alter the respiratory functional tests (Figure S1). Demographic, clinical, pharmacological and laboratory data were extracted from the electronic medical records and introduced in a REDCap database. Incoherent or missing data were identified and reviewed by experienced researchers. Publicly available whole blood RNA-sequencing (https://www.ncbi.nlm.nih.gov/geo/GSE228320) (García-Hidalgo, Peláez, et al., 2022) and plasma proteomic datasets (https://zenodo.org/record/8375667) (García-Hidalgo, González, Benítez, Carmona, Santisteve, Moncusí-Moix, et al., 2022) were used in the validation studies.

The study protocol was approved by the medical ethics committee of Hospital Universitari Arnau de Vilanova (CEIC/2273). The study was performed in full compliance with the Declaration of Helsinki (World Medical Association, 2013). The patients were provided with written information about the nature and goals of the study and signed an informed consent form.

2.2 | Pulmonary evaluation

A complete pulmonary evaluation was performed as previously detailed (González et al., 2021, 2022, 2023). Patients with diffusion impairment in the short-term visit (median [P_{25}; P_{75}] of 94.0 [83.8;105] days after hospital discharge) entered in the follow-up. Those patients that attended the long-term visit (median [P_{25}; P_{75}] of 358 [302;379] days after hospital discharge) completed the study population. In brief, the consultation comprised the assessment of general and respiratory symptoms, chest computed tomography and a 6-min walking test (6MWT). Respiratory function (diffusion capacity and lung volumes) was evaluated using a flow spirometer (MasterScreen, Jaeger, Germany) in agreement with the guidelines of the American Thoracic Society (ATS) (Celli et al., 2004). D_{LCO} was calculated as a percentage of the predicted D_{LCO} value according to the European Community Lung Health Survey (Roca et al., 1998). Lung diffusion impairment was defined as a D_{LCO} value under 80% of predicted, based on ATS/ERS task force: standardization of lung function testing (Pellegrino et al., 2005).

Patients who completed the 1-year follow-up were stratified, taking into consideration the persistence of diffusion impairment in the long-term visit: (i) "Recovery" (D_{LCO} ≥ 80% of predicted); (ii) "Persistence" (D_{LCO} < 80% of predicted).

2.3 | Plasma microRNA profiling

Plasma samples were processed under standardized conditions with support from the IRBLleida Biobank (B.000682) and Biobank and Biomodels Platform ISCIII PT20/00021. Venous blood samples were collected by venipuncture in EDTA tubes (BD, NJ, USA) after a night of fasting and before beginning the pulmonary evaluation at the short-term visit. Blood samples were centrifuged at 1500 × *g* for 10 min at

14765381, 0, Downloaded from https://bpspubs.onlinelibrary.wiley.com/doi/10.1111/bph.16330 by Universidad de la Rioja, Wiley Online Library on [14/03/2024]. See the Terms and Conditions (https://onlinelibrary.wiley.com/terms-and-conditions) on Wiley Online Library for rules of use; OA articles are governed by the applicable Creative Commons License

room temperature. Plasma supernatant was immediately aliquoted and stored at −80°C.

Total RNA was isolated from 200 µl of frozen plasma using the miRNeasy Serum/Plasma Advanced kit (Qiagen, Hilden, Germany). As a normalization strategy, synthetic *Caenorhabditis elegans* miR-39-3p (cel-miR-39-3p) was added as an external reference miRNA (1.6×10^8 copies per microlitre). The mixture was supplemented with 1 µg of MS2 carrier RNA (Roche Diagnostics, Mannheim, Germany) to improve extracellular miRNA yielding. The RNA Spike-In Kit (UniSp2, UniSp4 and UniSp5) (Qiagen, Hilden, Germany) was added as quality control of the RNA isolation. All reagents were spiked into samples during RNA isolation after incubation with the denaturing solution. The isolated RNA was eluted in 20 µl of RNAse-free water and stored at −80°C.

miRNA quantification was performed in agreement with the protocol from the miRCURY LNA Universal RT microRNA PCR System (Qiagen, Hilden, Germany). Reverse transcription (RT) to synthesize complementary DNA (cDNA) was conducted using a miRCURY LNA RT Kit (Qiagen, Hilden, Germany) in a total reaction volume of 10 µl. The spike-in UniSp6 (Qiagen, Hilden, Germany) was added to monitor the RT reaction. The RT conditions were the following: incubation at 42°C during 60 min, inactivation at 95°C during 5 min and immediate cooling at 4°C. Then, cDNA was kept at −20°C. A 41-miRNA panel, including mediators associated with mechanistic pathways altered in COVID-19 and its respiratory sequelae (de Gonzalo-Calvo et al., 2021), was quantified using miRCURY LNA miRNA Custom Panels (384-well plates) (Qiagen, Hilden, Germany). qPCR was performed with the QuantStudio™ 7 Flex Real-Time PCR System (Applied Biosystems, Waltham, MA, USA) in a volume of 10 µl. RT-qPCR conditions were 95°C during 2 min, 40 cycles of 95°C during 10 s followed by 56°C during 1 min and melting curve analysis. Synthetic UniSp3 was used as an interplate calibrator and qPCR control. Amplification curves were assessed using QuantStudio Software v1.3 (Thermo Fisher Scientific, Massachusetts, USA). The presence of single products and the absence of primer dimer was corroborated by melting curve analysis.

The quantification cycle (Cq) was defined as the fractional cycle number at which the fluorescence exceeded a given threshold. The Cq values of spike-in RNA templates were first analysed to monitor the homogenous efficiencies of RNA extraction procedures, the robustness of RT and the absence of PCR inhibitors. The ratio ΔCq (miR-23a-3p − miR-451a) proposed by Blondal et al. (2013) was used to exclude haemolysed samples. Cqs above 35 cycles were considered undetectable and censored at the minimum level observed for each miRNA. Relative quantification was performed using the $2^{-\Delta Cq}$ method ($\Delta Cq = Cq_{miRNA} - Cq_{cel\text{-}miR\text{-}39\text{-}3p}$). Expression levels were log-transformed for statistical analysis.

2.4 | Data and statistical analysis

The statistical analyses were performed using R software, version 4.1.2. Statistical analysis was undertaken only for studies where each group size was at least n = 5 and using independent values, that is, not treating technical replicates as independent values. Outlier analysis was conducted to identify incoherent data. Following thorough examination by experienced researchers, no outliers were excluded in the subsequent analysis. Descriptive statistics were used to outline the characteristics of the study population. The normality of the data was assessed using the Shapiro–Wilks test. Continuous variables were compared between groups using either the Mann–Whitney *U*-test or Student's *t* test, as appropriate, while categorical variables were compared using Fisher's exact test or chi-squared test. Data were presented as frequencies (percentage) for categorical variables and as medians [25th;75th percentile] or means (SD) for continuous variables. Pearson correlation was used to estimate the correlation between miRNAs. Differential gene expression analysis was conducted using the DESeq2 package (Love et al., 2014). Differences in protein levels were analysed using linear models with Empirical Bayes statistics (Ritchie et al., 2015). The *P*-value threshold defining statistical significance was set at <0.05.

miRNAs associated with persistent lung diffusion impairment were identified using a consensus of four supervised machine learning feature selection techniques with the intersection among the methods selected as the candidate miRNAs. A prior filtration step was performed to eliminate redundant information by removing miRNAs highly correlated to each other (cutoff Pearson correlation coefficient [PCC] > 0.7).

- *Random Forest by Boruta*: Boruta is a variable selection wrapper algorithm that employs random forest (RF) as the classification method (Kursa & Rudnicki, 2010). Boruta compared the importance of miRNAs to the importance of artificial shadow attributes, which were created by shuffling the original ones. The algorithm performed an iterative process (50 runs) that retained only those miRNAs exhibiting a higher importance value than their shadow counterparts. Finally, the attributes selected in any of the runs were incorporated. The method's classification performance was evaluated using a fivefold cross-validation (repeated 10 times) on a RF model. The number of variables randomly sampled as candidates at each split and the number of trees were set to their optimal values.
- *Random Forest by VSURF*: VSURF is a stepwise feature selection process based on RF (Genuer et al., 2015). The algorithm comprised three steps: (i) elimination of miRNAs with low importance by ranking the average of the variable importance measures in 50 runs of RF; (ii) calculation of the Out-of-bag (OOB) error rates for 50 RF runs for each nested model. The miRNAs with the lowest OOB error rates were selected; (iii) selection of the final model was performed by conducting an ascending sequence of RF tests that considered the inclusion of each miRNA to remove the most redundant ones. The performance of the selected miRNAs was assessed in a manner similar to the Boruta algorithm.
- *Relaxed Least Absolute Shrinkage and Selection Operator (LASSO)*: LASSO is a regression analysis method that selects variables by fitting a regularized least squares model (Fonti & Belitser, 2017). It penalized the regression coefficients, shrinking some of them to zero. The miRNAs with nonzero coefficients after the shrinkage

14765381, 0, Downloaded from https://bpspubs.onlinelibrary.wiley.com/doi/10.1111/bph.16330 by Universidad de la Rioja, Wiley Online Library on [14/03/2024]. See the Terms and Conditions (https://onlinelibrary.wiley.com/terms-and-conditions) on Wiley Online Library for rules of use; OA articles are governed by the applicable Creative Commons License

were selected for inclusion in the model. The lambda parameter (λ), which determines the strength of the penalty, was calculated through fivefold cross-validation. λ was selected as the value associated with the standard error greater than the minimum misclassification error. The variables were standardized before fitting the model. The model's performance was assessed using a 5-fold cross-validation (repeated 10 times).

- *Sparse partial least squares regression (sPLS)*: sPLS is a dimension reduction method that decomposes data matrices into component scores by imposing an L_1 penalty (Lê Cao et al., 2008). The method selected miRNAs while considering the LASSO penalty on the loading vectors estimated by partial least squares regression. A fivefold cross-validation was conducted to calculate optimal values for the sparsity parameters and the number of components in the final model.

The manuscript complies with *BJP*'s recommendations and requirements on experimental design and analysis (Curtis et al., 2022).

2.5 | Bioinformatics

Experimentally validated miRNA-gene interactions were extracted from TarBase v8 (Karagkouni et al., 2018). The search settings were restricted to interactions annotated from human, with Ensembl Gene IDs and from robust methods directly assessing miRNA binding. Protein–protein interaction (PPI) networks were constructed using the Search Tool for the Retrieval of Interacting Genes/Proteins database (STRING) (Szklarczyk et al., 2021). The minimum required interaction score was set at 0.900 (highest confidence). The functional enrichment analysis of the downstream target genes was conducted using the clusterProfiler 4.0 R package (Wu et al., 2021). ClusterProfiler library is embedded with updated annotations, such as Gene Ontology (GO), Kyoto Encyclopedia of Genes and Genomes (KEGG) and Reactome, among others. The *q* value (false discovery rate [FDR] adjusted *P* value) threshold was set at <0.05. Lung cell expression patterns were defined using data from the Genotype-Tissue Expression (GTEx) Portal (https://www.gtexportal.org/home/). The Drug-Gene Interaction database (DGIdb v4.2.0) was used to predict interactions between FDA-approved drugs and miRNA targets (Freshour et al., 2021).

2.6 | Materials

Details of materials and suppliers are provided in specific subsections in Methods.

2.7 | Nomenclature of targets and ligands

Key protein targets in this article are hyperlinked to corresponding entries in https://www.guidetopharmacology.org, and are permanently archived in the Concise Guide to PHARMACOLOGY 2021/22(151–157).

3 | RESULTS

Among the 119 survivors of critical COVID-19 included in the study, 84% exhibited impaired lung diffusion (D_{LCO} < 80% of predicted) at the short-term evaluation after hospital discharge. This group of patients entered in the follow-up study. No significant differences were reported between patients included in the study and those unreachable to attend the follow-up, except for the respiratory profile at the short-term visit (Table S1). One year after hospital discharge, D_{LCO} remained abnormal in 54.4% of these patients. Survivors with persistent diffusion impairment 1 year after discharge were older, had longer hospital and ICU stays and were more subjected to invasive mechanical ventilation (IMV) and prone positioning (Table 1). In the short-term visit, this group demonstrated significantly worse profiles concerning pulmonary function parameters, functional capacity and radiological findings (Table 2). As expected, a higher prevalence of diffusion impairment was observed in the long-term visit (Table 3), despite the improvement in the D_{LCO} levels during the follow-up (Figure S2).

Our initial objective was to identify miRNAs associated with persistent lung dysfunction, defined as D_{LCO} < 80% of predicted, 1 year after hospital discharge. To do that, we developed a feature selection process that combined four supervised machine learning-based methods with the circulating levels of miRNAs quantified at the short-term visit after hospital discharge. Because miRNAs could provide extremely redundant information, we undertook a prior filtration step, discarding those candidates highly correlated to each other (PCC > 0.7) (Figure S3). This step reduced the number of initial miRNAs to 12. The feature subset selected by Boruta and LASSO were similar (miR-9-5p and miR-486-5p) and different to the subsets provided by VSURF (miR-9-5p, miR-122-5p, miR-199a-5p, miR-214-3p and miR-486-5p) and sPLS (miR-9-5p, miR-214-3p and miR-486-5p) (Figure 1a). miR-9-5p and miR-486-5p were consistently selected by all four methods. An additional analysis was performed including those survivors who required the use of IMV during ICU stay. This subgroup of patients was considerably more homogenous in terms of both sociodemographic and clinical characteristics (Table S2). miR-486-5p was selected by Boruta, VSURF and sPLS (Figure S4).

Further evidence into the role of miRNAs in the pathogenesis of the respiratory sequelae and possible therapeutic candidates was evaluated through the analysis of the miRNA targets. The genes regulated by miR-9-5p and miR-486-5p were retrieved using experimentally validated miRNA-target interactions from DIANA-TarBase v8. The targetome of both miRNAs was composed by 1473 genes (1249 targets for miR-9-5p and 283 targets for miR-486-5p, with 59 targets in common) (Table S2). The interactions between the complete subset of genes were analysed using the STRING database. Supporting the complex gene expression network associated with miRNA biology,

14765381, 0, Downloaded from https://bpspubs.onlinelibrary.wiley.com/doi/10.1111/bph.16330 by Universidad de la Rioja, Wiley Online Library on [14/03/2024]. See the Terms and Conditions (https://onlinelibrary.wiley.com/terms-and-conditions) on Wiley Online Library for rules of use; OA articles are governed by the applicable Creative Commons License

TABLE 1 Sociodemographic, clinical and hospitalization characteristics based on the persistence of pulmonary dysfunction after 1 year of follow-up.

	All n = 57	Recovery n = 26	Persistence n = 31	*P* value	n
Sociodemographic characteristics					
Age (years)	62.0 [50.0;67.0]	57.0 [47.2;62.0]	63.0 [57.0;68.0]	0.021	57
Female	16 (28.1%)	9 (34.6%)	7 (22.6%)	0.477	57
BMI ($kg \cdot m^{-2}$)	28.7 [26.1;32.9]	28.2 [25.1;31.0]	29.3 [26.8;33.1]	0.396	57
Smoking history				0.193	57
Former	29 (50.9%)	11 (42.3%)	18 (58.1%)		
Nonsmoker	26 (45.6%)	13 (50.0%)	13 (41.9%)		
Current	2 (3.51%)	2 (7.69%)	0 (0.00%)		
Clinical characteristics					
Hypertension	31 (54.4%)	12 (46.2%)	19 (61.3%)	0.381	57
Type II diabetes mellitus	12 (21.1%)	4 (15.4%)	8 (25.8%)	0.525	57
Obesity	23 (40.4%)	8 (30.8%)	15 (48.4%)	0.280	57
Cardiovascular disease	3 (5.26%)	1 (3.85%)	2 (6.45%)	1.000	57
Chronic lung disease	1 (1.75%)	0 (0.00%)	1 (3.23%)	1.000	57
Asthma	5 (8.77%)	3 (11.5%)	2 (6.45%)	0.651	57
Chronic kidney disease	1 (1.75%)	0 (0.00%)	1 (3.23%)	1.000	57
ICU stay					
Time since first symptoms to ICU admission (days)	8.50 [7.00;10.0]	9.00 [8.00;10.0]	8.00 [6.50;10.0]	0.270	56
Time since hospital admission to ICU admission (days)	1.00 [0.00;3.00]	3.00 [1.00;4.00]	0.00 [0.00;2.00]	0.007	56
Hospital stay (days)	24.0 [15.0;39.0]	16.0 [11.2;30.2]	30.0 [23.0;44.5]	0.015	57
ICU stay (days)	14.0 [6.00;30.2]	6.00 [5.00;22.0]	16.0 [11.0;32.0]	0.006	56
Worst PaO_2/FiO_2 (mmHg)	134 [90.0;186]	137 [91.0;156]	118 [89.5;206]	0.987	57
PaO_2/FiO_2 categories				0.313	57
PaO_2/FiO_2 201–300 mmHg	13 (22.8%)	4 (15.4%)	9 (29.0%)		
PaO_2/FiO_2 101–200 mmHg	23 (40.4%)	13 (50.0%)	10 (32.3%)		
$PaO_2/FiO_2 \leq 100$ mmHg	21 (36.8%)	9 (34.6%)	12 (38.7%)		
High-flow nasal cannula	37 (64.9%)	18 (69.2%)	19 (61.3%)	0.729	57
Invasive mechanical ventilation	33 (57.9%)	9 (34.6%)	24 (77.4%)	0.003	57
Invasive mechanical ventilation duration (days)	18.0 [9.75;31.2]	23.0 [17.0;32.0]	16.0 [9.50;30.0]	0.529	32
Noninvasive mechanical ventilation	33 (57.9%)	12 (46.2%)	21 (67.7%)	0.169	57
Noninvasive mechanical ventilation duration (days)	3.00 [2.00;5.00]	3.00 [2.00;4.25]	3.00 [2.00;6.00]	0.372	33
Prone positioning	32 (56.1%)	8 (30.8%)	24 (77.4%)	0.001	57
Prone positioning duration (hours)	41.0 [23.0;75.0]	37.5 [23.5;91.5]	41.0 [22.5;70.0]	0.701	31
Antibiotics	49 (86.0%)	21 (80.8%)	28 (90.3%)	0.448	57
Hydroxychloroquine	25 (43.9%)	10 (38.5%)	15 (48.4%)	0.628	57
Tocilizumab	28 (49.1%)	10 (38.5%)	18 (58.1%)	0.227	57
Corticoids	49 (86.0%)	21 (80.8%)	28 (90.3%)	0.448	57
Remdesivir	13 (22.8%)	6 (23.1%)	7 (22.6%)	1.000	57
Interferon beta	12 (22.2%)	5 (20.8%)	7 (23.3%)	1.000	54
Lopinavir/ritonavir	25 (43.9%)	10 (38.5%)	15 (48.4%)	0.628	57
Anticoagulants	55 (96.5%)	25 (96.2%)	30 (96.8%)	1.000	57
Complications					
Bacterial pneumonia	6 (10.5%)	1 (4.00%)	5 (15.6%)	0.215	57
Pulmonary thromboembolism	2 (3.51%)	1 (4.00%)	1 (3.12%)	1.000	57
Bacteraemia	16 (28.1%)	4 (16.0%)	12 (37.5%)	0.135	57

14765381, 0, Downloaded from https://bpspubs.onlinelibrary.wiley.com/doi/10.1111/bph.16330 by Universidad de la Rioja, Wiley Online Library on [14/03/2024]. See the Terms and Conditions (https://onlinelibrary.wiley.com/terms-and-conditions) on Wiley Online Library for rules of use; OA articles are governed by the applicable Creative Commons License

TABLE 1 (Continued)

	All n = 57	Recovery n = 26	Persistence n = 31	*P* value	n
Acute kidney injury	16 (28.1%)	5 (20.0%)	11 (34.4%)	0.367	57
Liver dysfunction	10 (17.5%)	2 (8.00%)	8 (25.0%)	0.160	57
Hyperglycaemia	24 (42.1%)	9 (36.0%)	15 (46.9%)	0.579	57
Infectious complication	16 (28.1%)	5 (20.0%)	11 (34.4%)	0.367	57
Treatments after discharge					
Rehabilitation at discharge	21 (38.2%)	9 (36.0%)	12 (40.0%)	0.980	55
Corticoids at discharge	17 (32.1%)	9 (36.0%)	8 (28.6%)	0.777	53

Note: Continuous variables are expressed as mean (SD) or median [P_{25};P_{75}]. Categorical variables are expressed as n (%).
Abbreviations: BMI, body mass index; FiO_2, fraction of inspired oxygen; ICU, intensive care unit; PaO_2, oxygen partial pressure.

the targetome exhibited a high-confidence protein–protein interaction network with 1484 interactions (Figure 1b). To explore the molecular mechanisms associated with the persistence of lung dysfunction, the 1473 genes were subjected to functional enrichment analysis. We identified 23 KEGG pathways, 111 Reactome pathways and 474 GO processes (Tables S3, S4, and S5). The top-ranked pathways and processes were associated with inflammation, angiogenesis, senescence, tissue repair and remodelling, cell migration and pathogenesis of infectious agents, among other mechanisms (Figure 1c–e).

While standard functional analyses can reveal meaningful biological features, several biases should be acknowledged (Garcia-Moreno & Carmona-Saez, 2020). Consequently, we sought to corroborate our findings using RNA-sequencing data derived from whole blood samples collected from survivors of critical COVID-19. The differential expression analysis included survivors with and without lung diffusion impairment 1 year after hospital discharge (median age = 62.0 [53.0;68.0] years, females = 29.4%, 76.5% with D_{LCO} < 80% of predicted 1 year after hospital discharge, samples collected at a median of 97.0 [85.0;106] days after hospital discharge). Among the target genes, six transcripts were up-regulated (PXDN, FAT1, **ITGA2**, MXRA7, RNF187, TMEM200A) and five down-regulated (**CHRM3**, NELL2, RAI14, **SLC24A2**, PPP1R9A) in survivors with persistent lung dysfunction (Figure 2a). Functional enrichment analysis of the differentially expressed targets identified six overlapping pathways and processes, including those associated with cell migration and tissue repair, such as focal adhesion, signalling by MET and L1CAM interactions (Figure 2b and Tables S6, S7, and S8).

To further explore the expression profile of miRNA targets in lung cells, we retrieved data from the GTEx project, revealing that all genes are expressed in lung epithelial cells, endothelial cells and fibroblasts, with variable expression levels in immune cells (Figure 2c). Subsequently, we examined the repositioning potential of up-regulated miRNA targets using the Drug-Gene Interaction database, identifying two FDA-approved drugs (**clopidogrel** and **aspirin**) targeting one gene, ITGA2.

In pursuance of identifying mediators that support these findings, a validation step was performed using plasma proteomic data comprising survivors of critical COVID-19 (median age = 62.0 [49.0;67.5] years, females = 29.0%, 54.8% with persistent pulmonary dysfunction 1 year after hospital discharge, samples collected at a median of 97.0 [90.5;106] days after hospital discharge). As shown in Figure 2d,e, the plasma levels of **PTN** (6618) and KIM1, from a total of 364 proteins, were elevated in survivors of critical COVID-19 with persistent diffusion impairment. No FDA-approved drugs targeting PTN or KIM1 were retrieved from the Drug-Gene Interaction database.

4 | DISCUSSION

The increasing survival rate of critically ill patients paradoxically exerts a profound impact on National Health Systems. Given the substantial number of individuals surviving severe-to-critical COVID-19, there is a pressing concern regarding the prevalence of chronic pulmonary sequelae and their associated societal and economic burdens. Within this context, the management of respiratory sequelae in survivors of severe respiratory infections remains hindered by the limited efficacy of approved treatments. The molecular underpinnings contributing to the persistence of pulmonary sequelae following SARS-CoV-2 infection remain unclear. The results of an in-depth analysis of pathobiological mechanisms are very well suited to dissect the molecular basis of the long-term pulmonary sequelae. The greater accessibility to relatively novel tools has facilitated the implementation of innovative approaches for sophisticated molecular phenotyping (Vanhaverbeke et al., 2022). Here, we employed miRNA profiling of plasma samples collected from critical COVID-19 survivors, alongside the integration of RNA-sequencing and proteomic data, machine learning feature selection methods and bioinformatics, to delineate the early mechanistic pathways linked to the persistence of lung dysfunction and to identify potential candidate drugs.

In the initial phase, we established an association between two specific miRNAs, miR-9-5p and miR-486-5p, measured in plasma samples shortly after hospital discharge (median = 3 months after hospital discharge), and long-term lung function impairment (median = 12 months after hospital discharge) using four distinct feature selection algorithms. miR-486-5p was consistently selected by different feature selection methods when considering survivors who required the use of IMV during ICU stay. This approach has been previously used to develop classifiers for diseases and identify

14765381, 0, Downloaded from https://bpspubs.onlinelibrary.wiley.com/doi/10.1111/bph.16330 by Universidad de la Rioja, Wiley Online Library on [14/03/2024]. See the Terms and Conditions (https://onlinelibrary.wiley.com/terms-and-conditions) on Wiley Online Library for rules of use; OA articles are governed by the applicable Creative Commons License

TABLE 2 Pulmonary assessment at the short-term visit.

	All n = 57	Recovery n = 26	Persistence n = 31	*P* value	n
Symptoms					
Dry cough	11 (20.0%)	2 (8.00%)	9 (30.0%)	0.091	55
Wet cough	9 (16.4%)	4 (16.0%)	5 (16.7%)	1.000	55
Dyspnoea				0.075	54
0	25 (46.3%)	14 (56.0%)	11 (37.9%)		
1	16 (29.6%)	9 (36.0%)	7 (24.1%)		
2	11 (20.4%)	2 (8.00%)	9 (31.0%)		
3	2 (3.70%)	0 (0.00%)	2 (6.90%)		
Muscular fatigue	11 (20.0%)	4 (16.0%)	7 (23.3%)	0.735	55
Pulmonary function					
FVC (%)	73.1 (14.2)	77.4 (10.6)	69.5 (15.9)	0.030	57
FEV_1 (%)	81.7 (17.0)	85.1 (13.2)	78.8 (19.4)	0.150	57
FEV_1/FVC	0.83 (0.06)	0.82 (0.06)	0.83 (0.06)	0.662	57
TLC (%)	79.6 (19.4)	86.6 (17.0)	73.7 (19.6)	0.011	55
D_{LCO} (% of predicted)	60.7 (11.0)	68.9 (7.22)	53.8 (8.59)	<0.001	57
D_{LCO}				<0.001	57
<60% of predicted	24 (42.1%)	2 (7.69%)	22 (71.0%)		
<80% of predicted	33 (57.9%)	24 (92.3%)	9 (29.0%)		
RV (%)	79.1 [66.2;95.6]	79.5 [71.4;87.2]	75.8 [57.8;100]	0.577	55
KCO (%)	83.3 [75.8;91.2]	82.9 [75.3;91.1]	83.4 [75.9;90.0]	0.879	57
6-min walking test					
Distance (m)	401 (99.7)	430 (89.8)	375 (102)	0.041	54
Oxygen saturation average (%)	96.0 [94.0;96.0]	96.0 [95.0;97.0]	95.0 [93.2;96.0]	0.023	55
Oxygen saturation initial (%)	96.0 [96.0;97.0]	97.0 [96.0;97.0]	96.0 [95.0;97.0]	0.209	55
Oxygen saturation final (%)	96.0 [94.0;96.0]	96.0 [95.0;97.0]	95.0 [94.0;96.0]	0.043	55
Oxygen saturation minimal (%)	94.0 [92.5;96.0]	95.0 [93.0;96.0]	94.0 [92.0;95.0]	0.101	55
Chest CT					
Density					
Ground-glass	34 (60.7%)	15 (60.0%)	19 (61.3%)	1.000	56
Mixed ground-glass	26 (46.4%)	11 (44.0%)	15 (48.4%)	0.954	56
Consolidation	14 (25.0%)	4 (16.0%)	10 (32.3%)	0.277	56
Lesions					
Reticular	20 (35.7%)	12 (48.0%)	8 (25.8%)	0.149	56
Fibrotic	27 (48.2%)	6 (24.0%)	21 (67.7%)	0.003	56
TSS score	7.88 (4.07)	5.64 (3.32)	9.68 (3.75)	<0.001	56

Note: Continuous variables are expressed as mean (SD) or median [P_{25};P_{75}]. Categorical variables are expressed as n (%).
Abbreviations: D_{LCO}, carbon monoxide diffusing capacity; FEV_1, forced expiratory volume during the first second; FVC, forced vital capacity; KCO, CO transfer coefficient; RV, residual volume; TLC, total lung capacity; TSS, total severity score.

pathogenetic regulators (Errington et al., 2021). Machine learning methods offer the advantage of capturing previously unknown multi-dimensional interactions between predictors and outcomes, providing an unbiased approach to detect novel biological features. This specially applies to miRNAs, because they regulate gene expression through complex, coordinated and collective networks, as reported above. The combination of different methods limits the number of selected miRNAs, enhancing confidence and reproducibility. Certainly, plasma levels of miR-9-5p have been previously associated with radiological abnormalities in survivors of severe COVID-19 (García-Hidalgo, González, Benítez, Carmona, Santisteve, Pérez-Pons, et al., 2022). miR-486-5p levels also have been linked with COVID-19 severity (de Gonzalo-Calvo et al., 2021) and intra-ICU mortality (de Gonzalo-Calvo et al., 2023). Both miRNAs have been associated with

14765381, 0, Downloaded from https://bpspubs.onlinelibrary.wiley.com/doi/10.1111/bph.16330 by Universidad de la Rioja, Wiley Online Library on [14/03/2024]. See the Terms and Conditions (https://onlinelibrary.wiley.com/terms-and-conditions) on Wiley Online Library for rules of use; OA articles are governed by the applicable Creative Commons License

TABLE 3 Pulmonary assessment at the long-term visit.

	All n = 57	Recovery n = 26	Persistence n = 31	*P* value	n
Symptoms					
Dry cough	16 (29.1%)	6 (24.0%)	10 (33.3%)	0.645	55
Wet cough	9 (16.4%)	2 (8.00%)	7 (23.3%)	0.160	55
Dyspnoea				<0.001	55
0	29 (52.7%)	20 (80.0%)	9 (30.0%)		
1	15 (27.3%)	0 (0.00%)	15 (50.0%)		
2	9 (16.4%)	4 (16.0%)	5 (16.7%)		
3	2 (3.64%)	1 (4.00%)	1 (3.33%)		
Muscular fatigue	10 (19.2%)	4 (16.0%)	6 (22.2%)	0.729	52
Pulmonary function					
FVC (%)	86.6 [78.8;102]	87.0 [82.2;103]	86.0 [75.7;96.5]	0.344	57
FEV_1 (%)	83.8 (15.3)	83.7 (12.0)	83.9 (17.8)	0.966	57
FEV_1/FVC	82.1 (6.14)	82.9 (6.77)	81.5 (5.59)	0.408	57
TLC (%)	81.0 [72.2;93.2]	83.8 [76.8;93.2]	73.5 [67.4;90.2]	0.094	42
D_{LCO} (% predicted)	74.9 (15.4)	87.9 (9.91)	63.9 (9.33)	<0.001	57
D_{LCO}				<0.001	57
<60% of predicted	11 (19.3%)	0 (0.00%)	11 (35.5%)		
<80% of predicted	20 (35.1%)	0 (0.00%)	20 (64.5%)		
RV (%)	82.2 (30.0)	83.7 (33.0)	80.6 (27.1)	0.744	42
KCO (%)	86.0 [74.0;97.0]	97.5 [87.5;103]	76.0 [68.5;85.0]	<0.001	57
6-min walking test					
Distance (m)	453 (96.0)	457 (87.8)	450 (104)	0.805	56
Oxygen saturation average (%)	96.0 [95.0;96.0]	96.0 [95.0;97.0]	96.0 [94.8;96.0]	0.311	54
Oxygen saturation initial (%)	96.0 [96.0;97.0]	96.5 [96.0;97.8]	96.0 [96.0;97.0]	0.385	55
Oxygen saturation final (%)	95.0 [94.0;96.0]	95.0 [94.2;97.0]	95.0 [94.0;96.0]	0.319	54
Oxygen saturation minimal (%)	94.5 [93.0;95.8]	95.0 [93.2;96.0]	94.0 [91.8;95.0]	0.223	54
Chest CT					
Density					
Ground-glass	25 (43.9%)	12 (46.2%)	13 (41.9%)	0.959	57
Mixed ground-glass	27 (47.4%)	8 (30.8%)	19 (61.3%)	0.042	57
Consolidation	4 (7.02%)	2 (7.69%)	2 (6.45%)	1.000	57
Lesions					
Reticular	29 (60.4%)	12 (54.5%)	17 (65.4%)	0.639	48
Fibrotic	11 (22.9%)	4 (18.2%)	7 (26.9%)	0.709	48
TSS score	5.00 [3.00;6.00]	3.50 [2.25;5.00]	5.00 [4.25;6.00]	0.074	48

Note: Continuous variables are expressed as mean (SD) or median [P_{25};P_{75}]. Categorical variables are expressed as n (%).
Abbreviations: D_{LCO}, carbon monoxide diffusing capacity; FEV_1, forced expiratory volume during the first second; FVC, forced vital capacity; KCO, CO transfer coefficient; RV, residual volume; TLC, total lung capacity; TSS, total severity score.

pathogenetic mechanisms involved in lung damage and repair. For example, miR-486-5p has been shown to promote acute lung injury by inducing an excessive inflammatory response and inhibiting apoptosis (Luo et al., 2020). Conversely, and in line with the complex biology of miRNAs, other studies have proposed miR-486-5p as a key regulator of cell survival in *in vitro* models of lung alveolar epithelial cells (Li et al., 2018) and anti-fibrotic mediator in pulmonary fibrosis (Ji et al., 2015). Similarly, miR-9-5p has been described as a suppressor of the profibrogenic transformation of fibroblasts and a regulator of organ fibrosis (Fierro-Fernández et al., 2015).

The precise mechanisms by which acute respiratory infections, including SARS-CoV-2, lead to persistent lung sequelae are not yet fully understood. Data from critically ill patients suggest that failure to resolve epithelial barrier dysfunction, inflammation and matrix

14765381, 0, Downloaded from https://bpspubs.onlinelibrary.wiley.com/doi/10.1111/bph.16330 by Universidad de la Rioja, Wiley Online Library on [14/03/2024]. See the Terms and Conditions (https://onlinelibrary.wiley.com/terms-and-conditions) on Wiley Online Library for rules of use; OA articles are governed by the applicable Creative Commons License

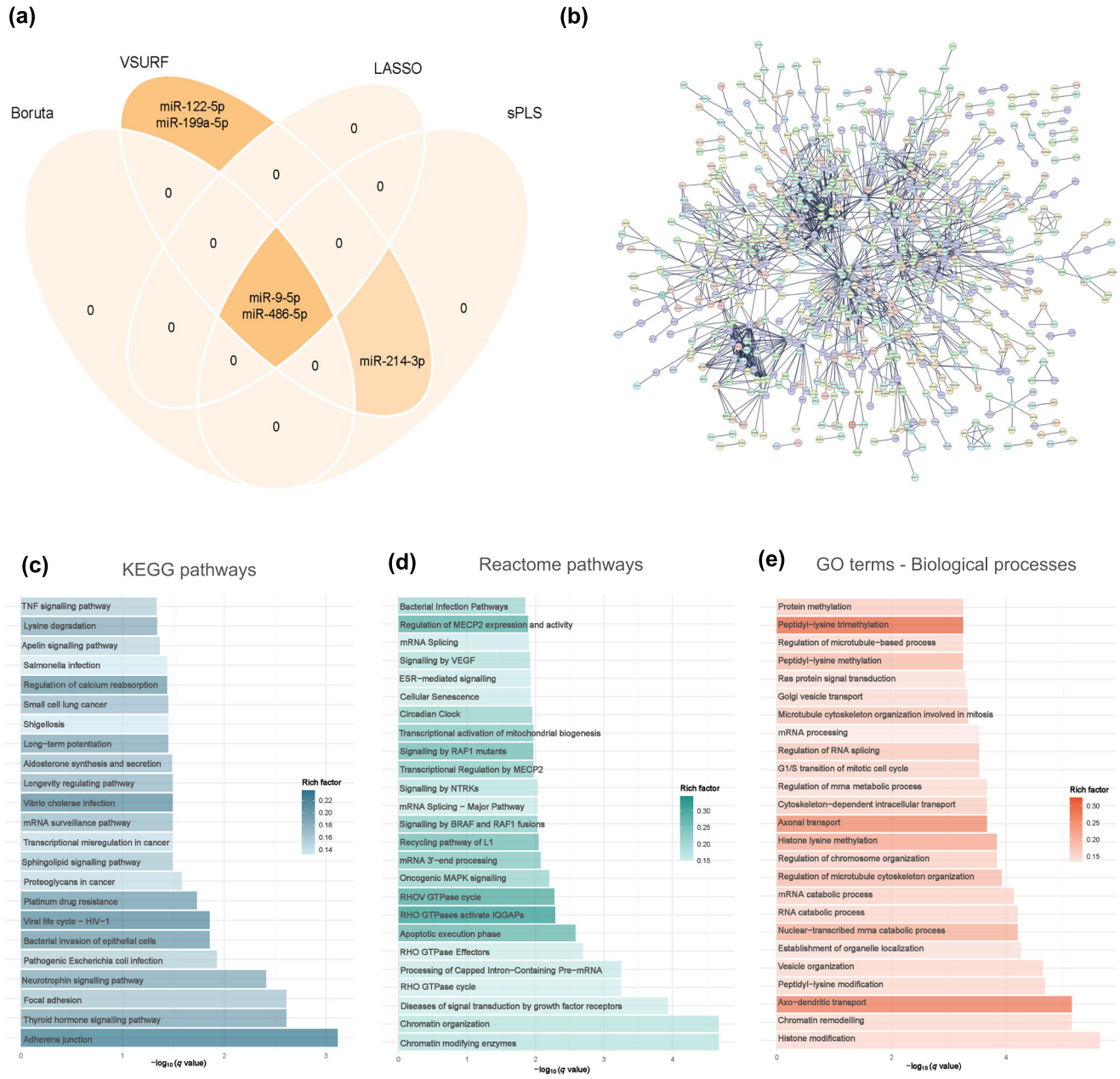

FIGURE 1 Molecular mechanisms associated with the persistence of diffusion impairment (D_{LCO} < 80% of predicted) 1 year after hospital discharge. (a) Identification of microRNAs associated with persistent lung diffusion impairment using a consensus of four supervised machine learning feature selection techniques (Boruta, VSURF, LASSO and sPLS) with the intersected miRNAs among the methods selected as candidates. (b) Protein–protein interaction (PPI) network using the experimentally validated target genes extracted from TarBase v8. The PPI network was constructed using STRING DB v12.0. (c–e) Functional enrichment analysis considering the downstream targetome using KEGG (c), Reactome (d) and GO (e) of the R package ClusterProfile 4.0. The plots show the *q* value (false discovery rate [FDR] adjusted *P* value) of the top 25 pathways. The intensity of the colours of the bars represents the rich factor, which denotes the ratio of target genes annotated in the molecular processes to all genes annotated in the processes.

remodelling, in addition to other processes such as coagulation, could result in chronic lung dysfunction (Martín-Vicente et al., 2021). In the case of COVID-19, accumulating evidence indicates that post-acute pulmonary lesions are driven by the interplay of multiple complex pathomechanisms. Treatable traits encompass inflammation, alveolar damage, endothelial injury, fibrosis, senescence, mitochondrial dysfunction and neutrophil recruitment (George et al., 2022; Pastor-Fernández et al., 2023; Sibila et al., 2022). The varied histological and immunohistochemical patterns observed in lung tissue from patients with pulmonary sequelae after COVID-19 support this notion (Ravaglia et al., 2022). The functional enrichment analysis performed in our study aligns with the existing literature, revealing an overrepresentation of pathways related to inflammation, angiogenesis and cell senescence, among others. Additionally, our supplementary

14765381, 0, Downloaded from https://bpspubs.onlinelibrary.wiley.com/doi/10.1111/bph.16330 by Universidad de la Rioja, Wiley Online Library on [14/03/2024]. See the Terms and Conditions (https://onlinelibrary.wiley.com/terms-and-conditions) on Wiley Online Library for rules of use; OA articles are governed by the applicable Creative Commons License

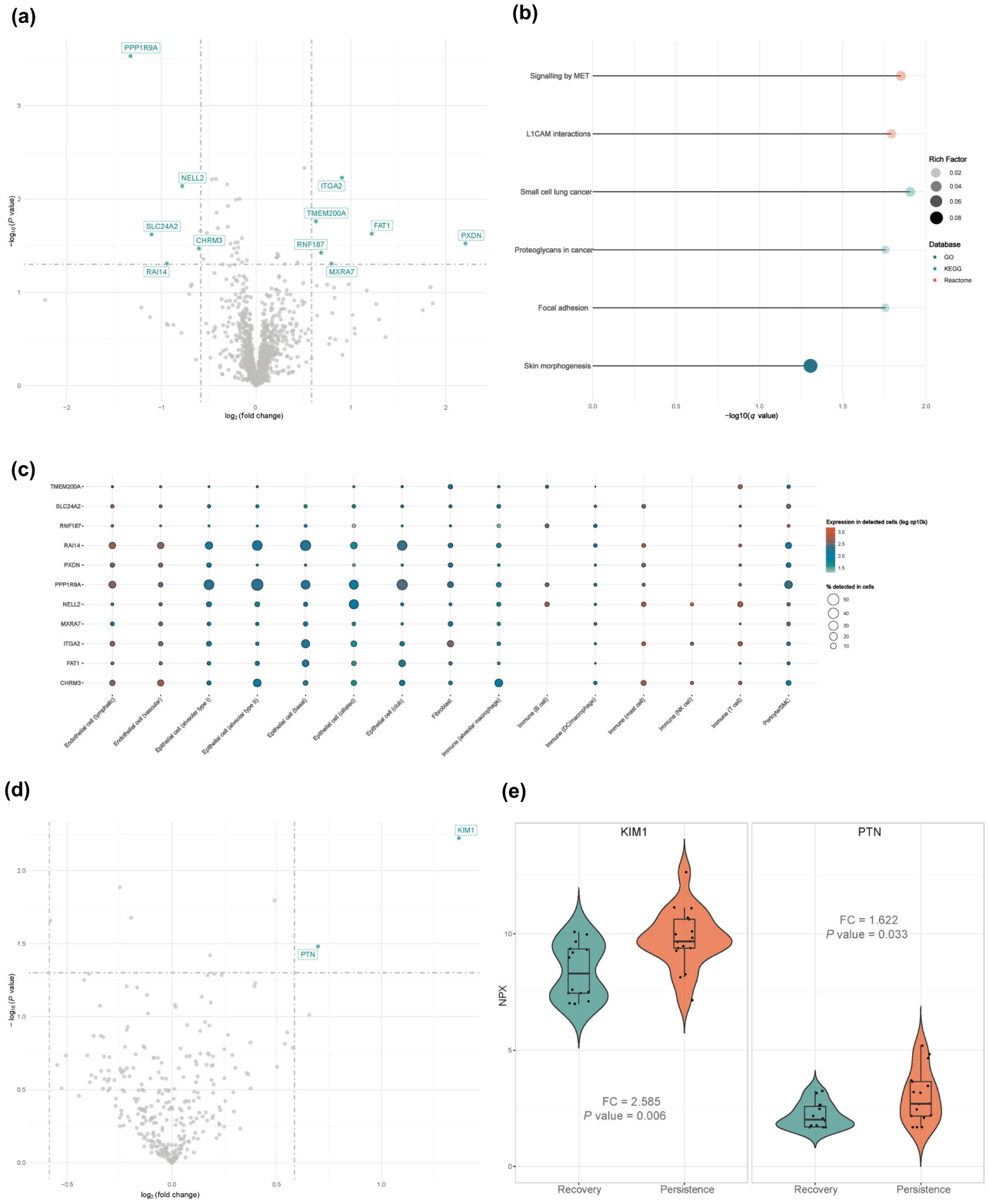

FIGURE 2 Legend on next page.

14765381, 0, Downloaded from https://bpspubs.onlinelibrary.wiley.com/doi/10.1111/bph.16330 by Universidad de la Rioja, Wiley Online Library on [14/03/2024]. See the Terms and Conditions (https://onlinelibrary.wiley.com/terms-and-conditions) on Wiley Online Library for rules of use; OA articles are governed by the applicable Creative Commons License

investigations indicate disruptions in pathways associated with cell migration and tissue repair as hallmark features of persistent lung dysfunction in critical COVID-19 survivors. These findings corroborate previous results from our group obtained through cross-sectional studies using diverse omics approaches (García-Hidalgo, González, Benítez, Carmona, Santisteve, Moncusí-Moix, et al., 2022; García-Hidalgo, Peláez, et al., 2022; Molinero, Gómez, et al., 2022). Furthermore, we have previously reported an association between elevated PTN and KIM1 levels, both of which play pivotal roles in tissue repair (Wang, 2020; Zhang & Cai, 2016), and severe diffusion impairment (D_{LCO} < 60% of predicted) 3 months after hospital discharge (García-Hidalgo, González, Benítez, Carmona, Santisteve, Moncusí-Moix, et al., 2022). Collectively, these findings have significant conceptual implications. At least at systemic level, respiratory sequelae are not a uniform entity but comprise diverse pathobiological mechanisms. This heterogeneity may pose a substantial barrier to improve patient management and could help explain the limited response to treatments and the negative outcomes of clinical trials. Comprehensive investigations are essential to maximize opportunities for developing novel therapeutics.

Our study provides valuable hypothesis-generating data from which to build future studies. The results suggest that there is a window of opportunity to prevent or treat long-term pulmonary damage in survivors of critical illness. Given the limited availability of treatments, miRNA-based therapeutics may represent a novel source of candidate drugs for addressing the persistence of lung dysfunction. In this regard, miRNA-based drugs have seen significant advances in the past decade and are considered a key technology in the therapeutic market (Bonneau et al., 2019). For instance, in the seminal study from Janssen et al. (2013), the administration of an antisense oligonucleotide that sequestered mature miR-122 to patients with chronic hepatitis C virus infection resulted in the reduction of the viral RNA levels. A recent investigation, combining different animal models and patient cohorts, reported that anti-miR-93-5p therapy prolonged sepsis survival through the regulation of both innate and adaptive immunity, that is, reducing the inflammatory monocytes and increasing circulating effector memory T cells (Dragomir et al., 2023). Another study also demonstrated the therapeutic efficacy of antisense therapy targeting miR-132-3p in various models of heart failure (Foinquinos et al., 2020). Supporting their potential transferability, a clinical trial phase 1b study suggested antisense therapy targeting miR-132-3p as safe and well tolerated (Täubel et al., 2021). miRNA mimic therapy also has provided promising results in bronchopulmonary dysplasia (Wen et al., 2021) and idiopathic pulmonary fibrosis (Chioccioli et al., 2022). Nevertheless, the safety of miRNA restoration therapy is still a matter of debate (Hong et al., 2020). Overall, these studies underscore the importance of considering miRNAs as potential therapeutic targets/agents. This becomes particularly relevant given the limited repositioning potential identified in our study. The drug–gene interaction analyses identified two FDA-approved drugs, clopidogrel and aspirin, targeting only one gene, ITGA2, thus not covering the entire spectrum of mechanisms associated with persistence. The limitations of miRNA-based therapeutics could be seen as an advantage, because the use of miRNAs that regulate multiple underlying pathways, traditionally considered an undesirable side effect, might prove beneficial in multifactorial conditions such as respiratory post-acute sequelae.

While our current investigation exhibits several strengths, including the use of a "real clinical context" with meticulous patient monitoring and comprehensive pulmonary assessments, it is imperative to acknowledge the limitations inherent to a pilot study. First, the relatively modest sample size may result in model overfitting. The study cohort was collected among SARS-CoV-2 patients during the early stages of the pandemic utilizing a single-centre design. The impact of potential confounding factors, such as age, sex or smoking status, should not be discarded. Nonetheless, differential expression analyses have been adjusted by these variables. Likewise, feature selection methods were applied to a more homogenous subgroup of critical survivors, showing consistent results. Further validation on external cohorts with more varied demographic and clinical characteristics and after sample size calculation are warranted. Whether our findings have an application in other post-acute patients deserves detailed investigations. To this end, we are currently collecting samples and data in a prospective manner (ClinicalTrials.gov Identifier: NCT06083363). Second, we have used a targeted strategy. However, we have selected miRNAs linked to mechanistic pathways implicated in lung disease, COVID-19 and its respiratory consequences. The present results offer robust support for the adoption of high-throughput technologies, such as sequencing. Third, additional studies are indispensable for dissecting the individual contributions of plasma miRNAs to the elucidated

FIGURE 2 Validation of the molecular mechanisms. (a) Volcano plot showing the *P*-value versus the fold change (FC) for the microRNA targets in the RNA sequencing dataset (n = 17). Green dots reflect significantly expressed genes considering a *P*-value <0.05 and a FC > 1.5 or FC < 0.66. (b) Functional enrichment analysis including the intersected molecular mechanisms after comparison of gene-set enrichment analysis using the whole targetome and using the validated target genes in the RNA sequencing dataset. The lollipop plot shows the *q* value of the pathways. The colours of the points displayed the distinct databases employed: GO, KEGG and Reactome. The intensity and size of the points represent the rich factor of each intersected biological process. (c) Cell enrichment analysis based on lung single-cell RNA-sequencing for the validated target genes using GTEx. Each column shows a cell type and each row represents a gene. The size of the point denotes the number of cells where the gene has been detected and the colour represents the expression level. The GTEx project was supported by the Common Fund of the Office of the Director of the National Institutes of Health and by the NCI, NHGRI, NHLBI, NIDA, NIMH and NINDS. (d) Volcano plot from proteomic dataset (n = 31) representing the *P*-value versus the fold change for each protein after comparison between recovered (D_{LCO} ≥ 80% of predicted) and persistent pulmonary dysfunction (D_{LCO} < 80% of predicted). Proteins with a *P*-value <0.05 and a FC > 1.5 or FC < 0.66 are depicted in green and considered as significant. (e) Violin plots of significant proteins. Inner boxplots show median and P_{25} and P_{75} ranges of expression values of each protein. FC and *P*-values are printed for each protein.

14765381, 0, Downloaded from https://bpspubs.onlinelibrary.wiley.com/doi/10.1111/bph.16330 by Universidad de la Rioja, Wiley Online Library on [14/03/2024]. See the Terms and Conditions (https://onlinelibrary.wiley.com/terms-and-conditions) on Wiley Online Library for rules of use; OA articles are governed by the applicable Creative Commons License

mechanistic pathways and their causal links to persistent lung dysfunction. Fourth, although patients with previous chronic pulmonary disease were excluded, we could not discard the presence of subclinical disease. Fifth, our findings align with a systemic impact of the respiratory sequelae. Previous investigations have suggested a compartmentalization of the lung concerning specific pathological mechanisms, particularly within the context of inflammation (Jouan et al., 2021). Furthermore, we have previously delineated disparities in the miRNA profiles observed in respiratory samples and plasma obtained from individuals with critical COVID-19 (de Gonzalo-Calvo et al., 2023; Molinero, Benítez, et al., 2022). Whether these mechanisms and potential targets are associated with organ dysfunction at the lung warrants further investigation. Sixth, we have not performed a biomarker study. While plasma miRNA profiles have traditionally been considered as a potential source of biomarkers, their utility as prognostic tools for managing pulmonary post-acute sequelae appears to be limited. The electronic health data provide enough information for prognostication. The group of patients with persistent diffusion impairment predominantly consists in older survivors with extended hospital and ICU stays, a higher need for IMV and prone positioning during the acute phase, diminished pulmonary function and capacity and an elevated prevalence of radiological abnormalities observed in the short-term follow-up visit after hospital discharge.

In conclusion, we successfully identified two miRNAs, miR-9-5p and miR-486-5p, linked to persistent lung dysfunction in survivors of critical COVID-19. Our findings provide a basis for understanding the intricate mechanistic pathways involved in the recovery of lung function. Current results offer promising avenues for the development of targeted disease-modifying agents to improve the long-term outcomes of individuals recovering from severe respiratory infections.

AUTHOR CONTRIBUTIONS

M.C. García-Hidalgo, I.D. Benítez, F. Barbé and D. de Gonzalo-Calvo were responsible for conceptualization. A. Torres, F Barbé and D. de Gonzalo-Calvo were involved in funding acquisition. F. Barbé and D. de Gonzalo-Calvo were in charge of project administration and supervision. Resources were organized and provided by J. González and D. de Gonzalo-Calvo. Data curation was performed by M.C. García-Hidalgo, M. Aguilà, S. Santisteve, A. Moncusí-Moix and C. Gort-Paniello. M.C. García-Hidalgo, M. Perez-Pons, M. Aguilà, S. Santisteve, R. Peláez and I.M. Larráyoz assisted with the investigation. Experimental methodology was done by M.C. García-Hidalgo, M. Perez-Pons and D. de Gonzalo-Calvo. M.C. García-Hidalgo, I.D. Benítez, R. Peláez, I.M. Larráyoz and D. de Gonzalo-Calvo contributed to formal analysis of the data. Software was developed by M.C. García-Hidalgo and I.D. Benítez. M.C. García-Hidalgo and M. Molinero were responsible for visualization of data. M.C. García-Hidalgo, I.D. Benítez and D. de Gonzalo-Calvo wrote the original draft. The review and editing of the manuscript were made by M. Perez-Pons, M. Molinero, T. Belmonte, C. Rodríguez-Muñoz, G. Torres, R. Peláez, I.M. Larráyoz, J. Caballero, C. Barberà, E. Nova-Lamperti, A. Torres, J. González, F. Barbé and D. de Gonzalo-Calvo.

ACKNOWLEDGEMENTS

This work supported by IRBLleida Biobank (B.000682) and Biobank and Biomodels Platform ISCIII PT20/00021. The human sample manipulation was performed in the Cell Culture Facility, Universitat de Lleida (Lleida, Catalonia, Spain).

CONFLICT OF INTEREST STATEMENT

The authors declare that they have no competing interests.

DATA AVAILABILITY STATEMENT

The data that support the findings of this study are available on request from the corresponding author. The external datasets were derived from the following resources available in the public domain: GEO (https://www.ncbi.nlm.nih.gov/geo/GSE228320) and Zenodo (https://zenodo.org/record/8375667).

DECLARATION OF TRANSPARENCY AND SCIENTIFIC RIGOUR

This Declaration acknowledges that this paper adheres to the principles for transparent reporting and scientific rigour of preclinical research as stated in the *BJP* guidelines for Design and Analysis and as recommended by funding agencies, publishers and other organizations engaged with supporting research.

REFERENCES

Bär, C., Thum, T., & de Gonzalo-Calvo, D. (2019). Circulating miRNAs as mediators in cell-to-cell communication. *Epigenomics*, *11*, 111–113. https://doi.org/10.2217/epi-2018-0183

Blondal, T., Jensby Nielsen, S., Baker, A., Andreasen, D., Mouritzen, P., Wrang Teilum, M., & Dahlsveen, I. K. (2013). Assessing sample and miRNA profile quality in serum and plasma or other biofluids. *Methods*, *59*, S1–S6. https://doi.org/10.1016/j.ymeth.2012.09.015

Bonneau, E., Neveu, B., Kostantin, E., Tsongalis, G. J., & De Guire, V. (2019). How close are miRNAs from clinical practice? A perspective on the diagnostic and therapeutic market. *EJIFCC*, *30*, 114–127.

Celli, B. R., MacNee, W., Agusti, A., Anzueto, A., Berg, B., Buist, A. S., Calverley, P. M. A., Chavannes, N., Dillard, T., Fahy, B., Fein, A., Heffner, J., Lareau, S., Meek, P., Martinez, F., McNicholas, W., Muris, J., Austegard, E., Pauwels, R., … ZuWallack, R. (2004). Standards for the diagnosis and treatment of patients with COPD: A summary of the ATS/ERS position paper. *European Respiratory Journal*, *23*, 932–946. https://doi.org/10.1183/09031936.04.00014304

Chioccioli, M., Roy, S., Newell, R., Pestano, L., Dickinson, B., Rigby, K., Herazo-Maya, J., Jenkins, G., Ian, S., Saini, G., Johnson, S. R., Braybrooke, R., Yu, G., Sauler, M., Ahangari, F., Ding, S., Deluliis, J., Aurelien, N., Montgomery, R. L., & Kaminski, N. (2022). A lung targeted miR-29 mimic as a therapy for pulmonary fibrosis. *eBioMedicine*, *85*, 104304. https://doi.org/10.1016/j.ebiom.2022.104304

Curtis, M. J., Alexander, S. P. H., Cirino, G., George, C. H., Kendall, D. A., Insel, P. A., Izzo, A. A., Ji, Y., Panettieri, R. A., Patel, H. H., Sobey, C. G., Stanford, S. C., Stanley, P., Stefanska, B., Stephens, G. J., Teixeira, M. M., Vergnolle, N., & Ahluwalia, A. (2022). Planning experiments: Updated guidance on experimental design and analysis and their reporting III. *British Journal of Pharmacology*, *179*, 3907–3913. https://doi.org/10.1111/bph.15868

Dragomir, M. P., Fuentes-Mattei, E., Winkle, M., Okubo, K., Bayraktar, R., Knutsen, E., Qdaisat, A., Chen, M., Li, Y., Shimizu, M., Pang, L., Liu, K., Liu, X., Anfossi, S., Zhang, H., Koch, I., Tran, A. M., Mohapatra, S.,

14765381, 0, Downloaded from https://bpspubs.onlinelibrary.wiley.com/doi/10.1111/bph.16330 by Universidad de la Rioja, Wiley Online Library on [14/03/2024]. See the Terms and Conditions (https://onlinelibrary.wiley.com/terms-and-conditions) on Wiley Online Library for rules of use; OA articles are governed by the applicable Creative Commons License

Ton, A., … Calin, G. A. (2023). Anti-miR-93-5p therapy prolongs sepsis survival by restoring the peripheral immune response. *The Journal of Clinical Investigation*, *133*, e158348. https://doi.org/10.1172/JCI158348

Errington, N., Iremonger, J., Pickworth, J. A., Kariotis, S., Rhodes, C. J., Rothman, A. M., Condliffe, R., Elliot, C. A., Kiely, D. G., Howard, L. S., Wharton, J., Thompson, A. A. R., Morrell, N. W., Wilkins, M. R., Wang, D., & Lawrie, A. (2021). A diagnostic miRNA signature for pulmonary arterial hypertension using a consensus machine learning approach. *eBioMedicine*, *69*, 103444. https://doi.org/10.1016/j.ebiom.2021.103444

Fierro-Fernández, M., Busnadiego, Ó., Sandoval, P., Espinosa-Díez, C., Blanco-Ruiz, E., Rodríguez, M., Pian, H., Ramos, R., López-Cabrera, M., García-Bermejo, M. L., & Lamas, S. (2015). miR-9-5p suppresses pro-fibrogenic transformation of fibroblasts and prevents organ fibrosis by targeting NOX4 and TGFBR2. *EMBO Reports*, *16*, 1358–1377. https://doi.org/10.15252/embr.201540750

Foinquinos, A., Batkai, S., Genschel, C., Viereck, J., Rump, S., Gyöngyösi, M., Traxler, D., Riesenhuber, M., Spannbauer, A., Lukovic, D., Weber, N., Zlabinger, K., Hašimbegović, E., Winkler, J., Fiedler, J., Dangwal, S., Fischer, M., De la Roche, J., Wojciechowski, D., … Thum, T. (2020). Preclinical development of a miR-132 inhibitor for heart failure treatment. *Nature Communications*, *11*, 633. https://doi.org/10.1038/s41467-020-14349-2

Fonti, V., & Belitser, E. (2017). Feature Selection using LASSO.

Freshour, S. L., Kiwala, S., Cotto, K. C., Coffman, A. C., McMichael, J. F., Song, J. J., Griffith, M., Griffith, O. L., & Wagner, A. H. (2021). Integration of the Drug-Gene Interaction Database (DGIdb 4.0) with open crowdsource efforts. *Nucleic Acids Research*, *49*, D1144–D1151. https://doi.org/10.1093/nar/gkaa1084

García-Hidalgo, M. C., González, J., Benítez, I. D., Carmona, P., Santisteve, S., Moncusí-Moix, A., Gort-Paniello, C., Rodríguez-Jara, F., Molinero, M., Perez-Pons, M., Torres, G., Caballero, J., Barberà, C., Tedim, A. P., Almansa, R., Ceccato, A., Fernández-Barat, L., Ferrer, R., Garcia-Gasulla, D., … CIBERESUCICOVID Project (COV20/00110, ISCIII). (2022). Proteomic profiling of lung diffusion impairment in the recovery stage of SARS-CoV-2-induced ARDS. *Clinical and Translational Medicine*, *12*, e838. https://doi.org/10.1002/ctm2.838

García-Hidalgo, M. C., González, J., Benítez, I. D., Carmona, P., Santisteve, S., Pérez-Pons, M., Moncusí-Moix, A., Gort-Paniello, C., Rodríguez-Jara, F., Molinero, M., Belmonte, T., Torres, G., Labarca, G., Nova-Lamperti, E., Caballero, J., Bermejo-Martin, J. F., Ceccato, A., Fernández-Barat, L., Ferrer, R., … on behalf of the CIBERESUCICOVID Project (COV20/00110, ISCIII). (2022). Identification of circulating microRNA profiles associated with pulmonary function and radiologic features in survivors of SARS-CoV-2-induced ARDS. *Emerging Microbes & Infections*, *11*, 1537–1549. https://doi.org/10.1080/22221751.2022.2081615

García-Hidalgo, M. C., Peláez, R., González, J., Santisteve, S., Benítez, I. D., Molinero, M., Perez-Pons, M., Belmonte, T., Torres, G., Moncusí-Moix, A., Gort-Paniello, C., Aguilà, M., Seck, F., Carmona, P., Caballero, J., Barberà, C., Ceccato, A., Fernández-Barat, L., Ferrer, R., … Larráyoz, I. M. (2022). Genome-wide transcriptional profiling of pulmonary functional sequelae in ARDS-secondary to SARS-CoV-2 infection. *Biomedicine & Pharmacotherapy*, *154*, 113617. https://doi.org/10.1016/j.biopha.2022.113617

Garcia-Moreno, A., & Carmona-Saez, P. (2020). Computational methods and software tools for functional analysis of miRNA data. *Biomolecules*, *10*, 1252. https://doi.org/10.3390/biom10091252

Genuer, R., Poggi, J.-M., & Tuleau-Malot, C. (2015). VSURF: An R package for variable selection using random forests. *The R Journal*, *7*, 19. https://doi.org/10.32614/RJ-2015-018

George, P. M., Reed, A., Desai, S. R., Devaraj, A., Faiez, T. S., Laverty, S., Kanwal, A., Esneau, C., Liu, M. K. C., Kamal, F., Man, W. D. C., Kaul, S., Singh, S., Lamb, G., Faizi, F. K., Schuliga, M., Read, J., Burgoyne, T., Pinto, A. L., … Singanayagam, A. (2022). A persistent neutrophil-associated immune signature characterizes post-COVID-19 pulmonary sequelae. *Science Translational Medicine*, *14*, eabo5795. https://doi.org/10.1126/scitranslmed.abo5795

de Gonzalo-Calvo, D., Benítez, I. D., Pinilla, L., Carratalá, A., Moncusí-Moix, A., Gort-Paniello, C., Molinero, M., González, J., Torres, G., Bernal, M., Pico, S., Almansa, R., Jorge, N., Ortega, A., Bustamante-Munguira, E., Gómez, J. M., González-Rivera, M., Micheloud, D., Ryan, P., … CIBERESUCICOVID Project (COV20/00110, ISCIII). (2021). Circulating microRNA profiles predict the severity of COVID-19 in hospitalized patients. *Translational Research*, *236*, 147–159. https://doi.org/10.1016/j.trsl.2021.05.004

de Gonzalo-Calvo, D., Molinero, M., Benítez, I. D., Perez-Pons, M., García-Mateo, N., Ortega, A., Postigo, T., García-Hidalgo, M. C., Belmonte, T., Rodríguez-Muñoz, C., González, J., Torres, G., Gort-Paniello, C., Moncusí-Moix, A., Estella, Á., Tamayo Lomas, L., Martínez de la Gándara, A., Socias, L., Peñasco, Y., … Barbé, F. (2023). A blood microRNA classifier for the prediction of ICU mortality in COVID-19 patients: A multicenter validation study. *Respiratory Research*, *24*, 159. https://doi.org/10.1186/s12931-023-02462-x

González, J., Benítez, I. D., Carmona, P., Santisteve, S., Monge, A., Moncusí-Moix, A., Gort-Paniello, C., Pinilla, L., Carratalá, A., Zuil, M., Ferrer, R., Ceccato, A., Fernández, L., Motos, A., Riera, J., Menéndez, R., Garcia-Gasulla, D., Peñuelas, O., Bermejo-Martin, J. F., … Trenado, J. (2021). Pulmonary function and radiologic features in survivors of critical COVID-19: A 3-month prospective cohort. *Chest*, *160*, 187–198. https://doi.org/10.1016/J.CHEST.2021.02.062

González, J., Zuil, M., Benítez, I. D., de Batlle, J., Aguilà, M., Santisteve, S., Varvará, N., Monge, A., Forns, N., Vaca, R., Minguez, O., Seck, F., Gort-Paniello, C., Moncusí-Moix, A., Caballero, J., Barberà, C., De Gonzalo-Calvo, D., Torres, A., Barbé, F., & CIBERESUCICOVID Project (COV20/00110, ISCIII). (2023). Long-term outcomes in critical COVID-19 survivors: A 2-year longitudinal cohort. *Archivos de Bronconeumología*, *59*, 691–697. https://doi.org/10.1016/j.arbres.2023.08.006

González, J., Zuil, M., Benítez, I. D., de Gonzalo-Calvo, D., Aguilar, M., Santisteve, S., Vaca, R., Minguez, O., Seck, F., Torres, G., De Batlle, J., Gómez, S., Barril, S., Moncusí-Moix, A., Monge, A., Gort-Paniello, C., Ferrer, R., Ceccato, A., Fernández, L., … Barbé, F. (2022). One year overview and follow-up in a post-COVID consultation of critically ill patients. *Frontiers in Medicine*, *9*, 897990. https://doi.org/10.3389/FMED.2022.897990

Herridge, M. S., Cheung, A. M., Tansey, C. M., Matte-Martyn, A., Diaz-Granados, N., al-Saidi, F., Cooper, A. B., Guest, C. B., Mazer, C. D., Mehta, S., Stewart, T. E., Barr, A., Cook, D., & Slutsky, A. S. (2003). One-year outcomes in survivors of the acute respiratory distress syndrome. *New England Journal of Medicine*, *348*, 683–693. https://doi.org/10.1056/nejmoa022450

Hong, D. S., Kang, Y.-K., Borad, M., Sachdev, J., Ejadi, S., Lim, H. Y., Brenner, A. J., Park, K., Lee, J. L., Kim, T. Y., Shin, S., Becerra, C. R., Falchook, G., Stoudemire, J., Martin, D., Kelnar, K., Peltier, H., Bonato, V., Bader, A. G., … Beg, M. S. (2020). Phase 1 study of MRX34, a liposomal miR-34a mimic, in patients with advanced solid tumours. *British Journal of Cancer*, *122*, 1630–1637. https://doi.org/10.1038/s41416-020-0802-1

Janssen, H. L. A., Reesink, H. W., Lawitz, E. J., Zeuzem, S., Rodriguez-Torres, M., Patel, K., Van der Meer, A. J., Patick, A. K., Chen, A., Zhou, Y., Persson, R., King, B. D., Kauppinen, S., Levin, A. A., & Hodges, M. R. (2013). Treatment of HCV infection by targeting microRNA. *The New England Journal of Medicine*, *368*, 1685–1694. https://doi.org/10.1056/NEJMoa1209026

Ji, X., Wu, B., Fan, J., Han, R., Luo, C., Wang, T., Yang, J., Han, L., Zhu, B., Wei, D., Chen, J., & Ni, C. (2015). The anti-fibrotic effects and mechanisms of MicroRNA-486-5p in pulmonary fibrosis. *Scientific Reports*, *5*, 14131. https://doi.org/10.1038/srep14131

14765381, 0, Downloaded from https://bpspubs.onlinelibrary.wiley.com/doi/10.1111/bph.16330 by Universidad de la Rioja, Wiley Online Library on [14/03/2024]. See the Terms and Conditions (https://onlinelibrary.wiley.com/terms-and-conditions) on Wiley Online Library for rules of use; OA articles are governed by the applicable Creative Commons License

Jouan, Y., Baranek, T., Si-Tahar, M., Paget, C., & Guillon, A. (2021). Lung compartmentalization of inflammatory biomarkers in COVID-19-related ARDS. *Critical Care*, *25*, 120. https://doi.org/10.1186/s13054-021-03513-9

Jusic, A., Thomas, P. B., Wettinger, S. B., Dogan, S., Farrugia, R., Gaetano, C., Tuna, B. G., Pinet, F., Robinson, E. L., Tual-Chalot, S., Stellos, K., Devaux, Y., & EU-CardioRNA COST Action CA17129. (2022). Noncoding RNAs in age-related cardiovascular diseases. *Ageing Research Reviews*, *77*, 101610. https://doi.org/10.1016/j.arr.2022.101610

Karagkouni, D., Paraskevopoulou, M. D., Chatzopoulos, S., Vlachos, I. S., Tastsoglou, S., Kanellos, I., Papadimitriou, D., Kavakiotis, I., Maniou, S., Skoufos, G., Vergoulis, T., Dalamagas, T., & Hatzigeorgiou, A. G. (2018). DIANA-TarBase v8: A decade-long collection of experimentally supported miRNA-gene interactions. *Nucleic Acids Research*, *46*, D239–D245. https://doi.org/10.1093/nar/gkx1141

Kerksieck, P., Ballouz, T., Haile, S. R., Schumacher, C., Lacy, J., Domenghino, A., Bauer, G. F., Dressel, H., Puhan, M. A., & Menges, D. (2023). Post COVID-19 condition, work ability and occupational changes in a population-based cohort. *The Lancet Regional Health Europe*, *31*, 100671. https://doi.org/10.1016/J.LANEPE.2023.100671

Kursa, M. B., & Rudnicki, W. R. (2010). Feature selection with the Boruta package. *Journal of Statistical Software*, *36*, 1–13. https://doi.org/10.18637/jss.v036.i11

Lê Cao, K.-A., Rossouw, D., Robert-Granié, C., & Besse, P. (2008). A sparse PLS for variable selection when integrating omics data. *Statistical Applications in Genetics and Molecular Biology*, *7*, 35. https://doi.org/10.2202/1544-6115.1390

Li, J., Salvador, A. M., Li, G., Valkov, N., Ziegler, O., Yeri, A., Yang Xiao, C., Meechoovet, B., Alsop, E., Rodosthenous, R. S., Kundu, P., Huan, T., Levy, D., Tigges, J., Pico, A. R., Ghiran, I., Silverman, M. G., Meng, X., Kitchen, R., … das, S. (2021). Mir-30d regulates cardiac remodeling by intracellular and paracrine signaling. *Circulation Research*, *128*, e1–e23. https://doi.org/10.1161/CIRCRESAHA.120.317244

Li, J., Zhou, Q., Liang, Y., Pan, W., Bei, Y., Zhang, Y., Wang, J., & Jiao, Z. (2018). miR-486 inhibits PM2.5-induced apoptosis and oxidative stress in human lung alveolar epithelial A549 cells. *Annals of Translational Medicine*, *6*, 209. https://doi.org/10.21037/atm.2018.06.09

Love, M. I., Huber, W., & Anders, S. (2014). Moderated estimation of fold change and dispersion for RNA-seq data with DESeq2. *Genome Biology*, *15*, 550. https://doi.org/10.1186/s13059-014-0550-8

Luo, Q., Zhu, J., Zhang, Q., Xie, J., Yi, C., & Li, T. (2020). MicroRNA-486-5p promotes acute lung injury via inducing inflammation and apoptosis by targeting OTUD7B. *Inflammation*, *43*, 975–984. https://doi.org/10.1007/s10753-020-01183-3

Makkos, A., Ágg, B., Petrovich, B., Varga, Z. V., Görbe, A., & Ferdinandy, P. (2021). Systematic review and network analysis of microRNAs involved in cardioprotection against myocardial ischemia/reperfusion injury and infarction: Involvement of redox signalling. *Free Radical Biology & Medicine*, *172*, 237–251. https://doi.org/10.1016/j.freeradbiomed.2021.04.034

Martín-Vicente, P., López-Martínez, C., Lopez-Alonso, I., López-Aguilar, J., Albaiceta, G. M., & Amado-Rodríguez, L. (2021). Molecular mechanisms of postintensive care syndrome. *Intensive Care Medicine Experimental*, *9*, 58. https://doi.org/10.1186/s40635-021-00423-6

Molinero, M., Benítez, I. D., González, J., Gort-Paniello, C., Moncusí-Moix, A., Rodríguez-Jara, F., García-Hidalgo, M. C., Torres, G., Vengoechea, J. J., Gómez, S., Cabo, R., Caballero, J., Bermejo-Martin, J. F., Ceccato, A., Fernández-Barat, L., Ferrer, R., Garcia-Gasulla, D., Menéndez, R., Motos, A., … De Gonzalo-Calvo, D. (2022). Bronchial aspirate-based profiling identifies MicroRNA signatures associated with COVID-19 and fatal disease in critically ill patients. *Frontiers in Medicine*, *8*, 756517. https://doi.org/10.3389/fmed.2021.756517

Molinero, M., Gómez, S., Benítez, I. D., Vengoechea, J. J., González, J., Polanco, D., Gort-Paniello, C., Moncusí-Moix, A., García-Hidalgo, M. C., Perez-Pons, M., Belmonte, T., Torres, G., Caballero, J., Barberà, C., Ayestarán Rota, J. I., Socías Crespí, L., Ceccato, A., Fernández-Barat, L., Ferrer, R., … De Gonzalo-Calvo, D. (2022). Multiplex protein profiling of bronchial aspirates reveals disease-, mortality- and respiratory sequelae-associated signatures in critically ill patients with ARDS secondary to SARS-CoV-2 infection. *Frontiers in Immunology*, *13*, 942443. https://doi.org/10.3389/fimmu.2022.942443

Mylvaganam, R. J., Bailey, J. I., Sznajder, J. I., & Sala, M. A. (2021). Recovering from a pandemic: Pulmonary fibrosis after SARS-CoV-2 infection. *European Respiratory Review*, *30*, 210194. https://doi.org/10.1183/16000617.0194-2021

Nalbandian, A., Sehgal, K., Gupta, A., Madhavan, M. V., McGroder, C., Stevens, J. S., Cook, J. R., Nordvig, A. S., Shalev, D., Sehrawat, T. S., Ahluwalia, N., Bikdeli, B., Dietz, D., der-Nigoghossian, C., Liyanage-Don, N., Rosner, G. F., Bernstein, E. J., Mohan, S., Beckley, A. A., … Wan, E. Y. (2021). Post-acute COVID-19 syndrome. *Nature Medicine*, *27*, 601–615. https://doi.org/10.1038/s41591-021-01283-z

Pastor-Fernández, A., Bertos, A. R., Sierra-Ramírez, A., del Moral-Salmoral, J., Merino, J., de Ávila, A. I., Olagüe, C., Villares, R., González-Aseguinolaza, G., Rodríguez, M. Á., Fresno, M., Gironés, N., Bustos, M., Smerdou, C., Fernandez-Marcos, P. J., & Von Kobbe, C. (2023). Treatment with the senolytics dasatinib/quercetin reduces SARS-CoV-2-related mortality in mice. *Aging Cell*, *22*, e13771. https://doi.org/10.1111/ACEL.13771

Pellegrino, R., Viegi, G., Brusasco, V., Crapo, R. O., Burgos, F., Casaburi, R., Coates, A., Van Der Grinten, C. P., Gustafsson, P., Hankinson, J., & Jensen, R. (2005). Interpretative strategies for lung function tests. *European Respiratory Journal*, *26*, 948–968. https://doi.org/10.1183/09031936.05.00035205

Ranieri, V. M., Rubenfeld, G. D., Thompson, B. T., Ferguson, N. D., Caldwell, E., Fan, E., & Camporota, L. (2012). Acute respiratory distress syndrome: The Berlin definition. *JAMA: The Journal of the American Medical Association*, *307*, 2526–2533. https://doi.org/10.1001/jama.2012.5669

Ravaglia, C., Doglioni, C., Chilosi, M., Piciucchi, S., Dubini, A., Rossi, G., Pedica, F., Puglisi, S., Donati, L., Tomassetti, S., & Poletti, V. (2022). Clinical, radiological and pathological findings in patients with persistent lung disease following SARS-CoV-2 infection. *The European Respiratory Journal*, *60*, 2102411. https://doi.org/10.1183/13993003.02411-2021

Ritchie, M. E., Phipson, B., Wu, D., Hu, Y., Law, C. W., Shi, W., & Smyth, G. K. (2015). limma powers differential expression analyses for RNA-sequencing and microarray studies. *Nucleic Acids Research*, *43*, e47. https://doi.org/10.1093/NAR/GKV007

Roca, J., Burgos, F., Sunyer, J., Saez, M., Chinn, S., Anto, J., Rodriguez-Roisin, R., Quanjer, P. H., Nowak, D., & Burney, P. (1998). References values for forced spirometry. Group of the European Community Respiratory Health Survey. *European Respiratory Journal*, *11*, 1354–1362. https://doi.org/10.1183/09031936.98.11061354

Rupani, H., Sanchez-Elsner, T., & Howarth, P. (2013). MicroRNAs and respiratory diseases. *European Respiratory Journal*, *41*, 695–705. https://doi.org/10.1183/09031936.00212011

Schlemmer, F., Valentin, S., Boyer, L., Guillaumot, A., Chabot, F., Dupin, C., Le Guen, P., Lorillon, G., Bergeron, A., Basille, D., Delomez, J., Andrejak, C., Bonnefoy, V., Goussault, H., Assié, J. B., Choinier, P., Ruppert, A. M., Cadranel, J., Mennitti, M. C., … RE2COVERI Study Group. (2023). Respiratory recovery trajectories after severe-to-critical COVID-19: A 1-year prospective multicentre study. *European Respiratory Journal*, *61*, 2201532. https://doi.org/10.1183/13993003.01532-2022

Sibila, O., Perea, L., Albacar, N., Moisés, J., Cruz, T., Mendoza, N., Solarat, B., Lledó, G., Espinosa, G., Barberà, J. A., Badia, J. R., Agustí, A., Sellarés, J., & Faner, R. (2022). Elevated plasma levels of epithelial and endothelial cell markers in COVID-19 survivors with reduced lung diffusing capacity six months after hospital discharge. *Respiratory Research*, *23*, 37. https://doi.org/10.1186/s12931-022-01955-5

14765381, 0, Downloaded from https://bpspubs.onlinelibrary.wiley.com/doi/10.1111/bph.16330 by Universidad de la Rioja, Wiley Online Library on [14/03/2024]. See the Terms and Conditions (https://onlinelibrary.wiley.com/terms-and-conditions) on Wiley Online Library for rules of use; OA articles are governed by the applicable Creative Commons License

Singh, S. J., Baldwin, M. M., Daynes, E., Evans, R. A., Greening, N. J., Jenkins, R. G., Lone, N. I., McAuley, H., Mehta, P., Newman, J., Novotny, P., Smith, D. J. F., Stanel, S., Toshner, M., & Brightling, C. E. (2023). Respiratory sequelae of COVID-19: Pulmonary and extrapulmonary origins, and approaches to clinical care and rehabilitation. *The Lancet Respiratory Medicine*, *11*, 709–725. https://doi.org/10.1016/S2213-2600(23)00159-5

Szklarczyk, D., Gable, A. L., Nastou, K. C., Lyon, D., Kirsch, R., Pyysalo, S., Doncheva, N. T., Legeay, M., Fang, T., Bork, P., Jensen, L. J., & Von Mering, C. (2021). The STRING database in 2021: Customizable protein-protein networks, and functional characterization of user-uploaded gene/measurement sets. *Nucleic Acids Research*, *49*, 605–612. https://doi.org/10.1093/nar/gkaa1074

Täubel, J., Hauke, W., Rump, S., Viereck, J., Batkai, S., Poetzsch, J., Rode, L., Weigt, H., Genschel, C., Lorch, U., Theek, C., Levin, A. A., Bauersachs, J., Solomon, S. D., & Thum, T. (2021). Novel antisense therapy targeting microRNA-132 in patients with heart failure: Results of a first-in-human phase 1b randomized, double-blind, placebo-controlled study. *European Heart Journal*, *42*, 178–188. https://doi.org/10.1093/eurheartj/ehaa898

Torres, A., Arguimbau, M., Bermejo-Martín, J., Campo, R., Ceccato, A., Fernandez-Barat, L., Ferrer, R., Jarillo, N., Lorente-Balanza, J. Á., Menéndez, R., Motos, A., Muñoz, J., Peñuelas Rodríguez, Ó., Pérez, R., Riera, J., Rodríguez, A., Sánchez, M., & Barbe, F. (2021). CIBERESUCI-COVID: Un proyecto estratégico para una mejor comprensión y manejo clínico de la COVID-19 en pacientes críticos. *Archivos de Bronconeumología*, *57*, 1–2. https://doi.org/10.1016/J.ARBRES.2020.10.021

Valadi, H., Ekström, K., Bossios, A., Sjöstrand, M., Lee, J., & Lötvall, J. (2007). Exosome-mediated transfer of mRNAs and microRNAs is a novel mechanism of genetic exchange between cells. *Nature Cell Biology*, *9*, 654–659. https://doi.org/10.1038/NCB1596

Vanhaverbeke, M., Attard, R., Bartekova, M., Ben-Aicha, S., Brandenburger, T., de Gonzalo-Calvo, D., Emanueli, C., Farrugia, R., Grillari, J., Hackl, M., Kalocayova, B., Martelli, F., Scholz, M., Wettinger, S. B., & Devaux, Y. (2022). Peripheral blood RNA biomarkers for cardiovascular disease from bench to bedside: A position paper from the EU-CardioRNA COST action CA17129. *Cardiovascular Research*, *118*, 3183–3197. https://doi.org/10.1093/cvr/cvab327

Wang, X. (2020). Pleiotrophin: Activity and mechanism. *Advances in Clinical Chemistry*, *98*, 51–89. https://doi.org/10.1016/bs.acc.2020.02.003

Wen, X., Zhang, H., Xiang, B., Zhang, W., Gong, F., Li, S., Chen, H., Luo, X., Deng, J., You, Y., Hu, Z., & Jiang, C. (2021). Hyperoxia-induced miR-342-5p down-regulation exacerbates neonatal bronchopulmonary dysplasia via the Raf1 regulator Spred3. *British Journal of Pharmacology*, *178*, 2266–2283. https://doi.org/10.1111/bph.15371

World Medical Association. (2013). World Medical Association Declaration of Helsinki: ethical principles for medical research involving human subjects. *JAMA*, *310*(20), 2191–2194. https://doi.org/10.1001/jama.2013.281053

Wu, T., Hu, E., Xu, S., Chen, M., Guo, P., Dai, Z., Feng, T., Zhou, L., Tang, W., Zhan, L., Fu, X., Liu, S., Bo, X., & Yu, G. (2021). clusterProfiler 4.0: A universal enrichment tool for interpreting omics data. *The Innovation*, *2*, 100141. https://doi.org/10.1016/j.xinn.2021.100141

Ying, W., Gao, H., Dos Reis, F. C. G., Bandyopadhyay, G., Ofrecio, J. M., Luo, Z., Ji, Y., Jin, Z., Ly, C., & Olefsky, J. M. (2021). MiR-690, an exosomal-derived miRNA from M2-polarized macrophages, improves insulin sensitivity in obese mice. *Cell Metabolism*, *33*, 781–790.e5. https://doi.org/10.1016/j.cmet.2020.12.019

Zhang, Z., & Cai, C. X. (2016). Kidney injury molecule-1 (KIM-1) mediates renal epithelial cell repair via ERK MAPK signaling pathway. *Molecular and Cellular Biochemistry*, *416*, 109–116. https://doi.org/10.1007/S11010-016-2700-7

SUPPORTING INFORMATION

Additional supporting information can be found online in the Supporting Information section at the end of this article.

How to cite this article: García-Hidalgo, M. C., Benítez, I. D., Perez-Pons, M., Molinero, M., Belmonte, T., Rodríguez-Muñoz, C., Aguilà, M., Santisteve, S., Torres, G., Moncusí-Moix, A., Gort-Paniello, C., Peláez, R., Larráyoz, I. M., Caballero, J., Barberà, C., Nova-Lamperti, E., Torres, A., González, J., Barbé, F., & de Gonzalo-Calvo, D. (2024). MicroRNA-guided drug discovery for mitigating persistent pulmonary complications in critical COVID-19 survivors: A longitudinal pilot study. *British Journal of Pharmacology*, 1–16. https://doi.org/10.1111/bph.16330

14765381, 0, Downloaded from https://bpspubs.onlinelibrary.wiley.com/doi/10.1111/bph.16330 by Universidad de la Rioja, Wiley Online Library on [14/03/2024]. See the Terms and Conditions (https://onlinelibrary.wiley.com/terms-and-conditions) on Wiley Online Library for rules of use; OA articles are governed by the applicable Creative Commons License